Acta Materialia 98 (2015) 318–326

Contents lists available at ScienceDirect

Acta Materialia

journal homepage: www.elsevier.com/locate/actamat

Ultra-high coercivity of $(Fe_{86-x}Nb_xB_{14})_{0.88}Tb_{0.12}$ bulk nanocrystalline magnets

A. Chrobak [a,*], G. Ziółkowski [a], N. Randrianantoandro [b], J. Klimontko [a], D. Chrobak [c], K. Prusik [c], J. Rak [c]

[a] Institute of Physics, University of Silesia, Uniwersytecka 4, 40-007 Katowice, Poland
[b] LUNAM Université – Université du Maine, Institut des Molécules et des Matériaux du Mans, UMR CNRS 6283, Avenue Olivier Messaien, 72085 Le Mans Cedex 9, France
[c] Institute of Materials Science, University of Silesia, 75 Pułku Piechoty 1, 41-500 Chorzów, Poland

ARTICLE INFO

Article history:
Received 28 April 2015
Revised 21 July 2015
Accepted 22 July 2015
Available online 8 August 2015

Keywords:
Hard magnets
Micromagnetism
Magnetic domains
Biphase magnetic systems

ABSTRACT

The paper refers to hard magnetic properties of $(Fe_{86-x}Nb_xB_{14})_{0.88}Tb_{0.12}$ bulk nanocrystalline magnets prepared using the vacuum mold suction technique. A combination of a specific chemical composition and sample preparation technology leads to a formation of dendrite grains of $Tb_2Fe_{14}B$ hard magnetic phase. The microstructure of the obtained alloys strongly depends on both these factors. The examined alloys reveal high and ultra-high coercivity exceeding 7 T at room temperature. It was shown that the observed magnetic hardening is caused by the shape of the dendrite grains with sub-micro branches as a source of additional exchange anisotropy. Favorable hard magnetic properties occur for the alloy with 6 at.% of Nb content which corresponds to the maximum of activation enthalpy of Fe crystallization in amorphous $Fe_{86-x}Nb_xB_{14}$ basic alloys.

1. Introduction

Hard magnetic materials find wide applications in modern technologies as permanent magnets in electric motors, generators, sensors, actuators or recording media in storage devices. Nowadays, alloys and compounds based on transition (TM) and rare earth (RE) elements are considered as the best, taking into account their coercive field H_c and energy product $|BH|_{max}$, which describe the stray field force [1–4]. For example, Nd–Fe–B based sintered magnets reach values of $\mu_0 H_c \approx 1.2$ T and $|BH|_{max} \approx 400$ kJ/m^3, meaning a relatively good magnetic stability and a strong stray magnetic field. These superb parameters are a consequence of magneto-crystalline anisotropy and high magnetic moment of the $Nd_2Fe_{14}B$ phase. In the case of sintered materials, additional magnetic anisotropies (shape and surface type) are introduced by preparation techniques. Properties of the $Nd_2Fe_{14}B$ phase have been known for over 30 years, but investigations of new hard magnetic materials are still important due to increasing demand for permanent magnets and limited natural resources of rare earths [5]. Therefore, the recent studies are focused on: (i) systems without RE (e.g. Fe–Pt, Co–Pt, MnBi, MnAlC alloys), (ii) improvement of Alnico (Al–Ni–Co–Fe) coercivity, and (iii) decrease of the RE content by exchange-coupled soft phases and additional magnetic anisotropy resulting from nano- or microstructure [6–10]. Formation of a preferred nanostructure can be supported by Nb as an alloying addition especially for systems starting from amorphous precursors. Indeed, as much as 4 at.% of niobium significantly improve hard magnetic properties of Nd–Fe–B based nanocrystalline alloys [11]. The other promising method of magnetic hardening is hot deformation leading to an introduction of additional magnetic anisotropy by micro-sized grains [12].

In the field of ultra-high coercive materials, alloys of Tb–Fe–B type are very promising. In fact, for $Tb_{14}Fe_{79.6}B_{6.4}$ nanocrystalline melt spun ribbons (thickness in the order of tens of μm), almost 8 T coercivity and a strong influence of the cooling rate on magnetic properties has been reported [13]. Despite this achievement, the form of strips narrows possible application down, as in many cases, bulk materials are required. One of the methods commonly used for preparation of bulk magnets is the so-called vacuum suction mold casting in which the melted material is rapidly quenched with a cooling rate in order of 10^3 K/s. Moreover, materials obtained by this technique usually contain nanocrystallites of different phases.

Recently, we have reported magnetic properties and magnetic hardening effect of $(Fe_{80}Nb_6B_{14})_{1-x}Tb_x$ $(0.02 \leqslant x \leqslant 0.32)$ bulk nanocrystalline alloys prepared by the mold casting [14,15]. These studies indicated that the used preparation method may yield bulk magnetic nanocomposite alloys in the form of rods with a diameter $d = 0.5 - 2$ mm. The alloys were composed of hard

* Corresponding author.
E-mail address: artur.chrobak@us.edu.pl (A. Chrobak).

http://dx.doi.org/10.1016/j.actamat.2015.07.056
1359-6454/

($Tb_2Fe_{14}B$), soft ($TbFe_2$, iron borides and α-Fe) ferromagnetic phases, and a paramagnetic phase ($Tb_{1.1}Fe_4B_4$). It is well established that the magnetic properties of such nanocomposites strongly depend on their chemical composition and the cooling rate controlled by the sample diameter. For $(Fe_{80}Nb_6B_{14})_{1-x}Tb_x$ alloys, a decrease in the sample diameter (an increase of the cooling rate) leads to a significant magnetic hardening. For the alloy with $x = 0.1$, the coercive field increases from 0.57 to 2.66 T (about 5 times), while the demagnetization energy $|JH|_{max}$ increases from 28.7 to 82.6 kJ/m^3 (about 3 times). The highest value of the coercive field (3.56 T) was observed for $x = 0.11$ and $d = 0.5$ mm. Is should be emphasized that all the examined samples were prepared with a value of melting current equal to 25 A, which in the present work is an important varying parameter. The values of $|JH|_{max}$, (where J is the magnetic polarization) determined from the $M(H)$ magnetization isotherm loops in the second quadrant, describe magnetic energy density stored in the material, which also means the energy required for demagnetization. This parameter, different from $|BH|_{max}$, indicates magnetic stability or resistance of materials to an external magnetic field. It is known that in the case of RE–Fe–B alloys, the stray field energy ($|BH|_{max}$) strongly depends on the type of the RE element, i.e., for a so-called light RE (Ce, Pr, Nd) is high due to ferromagnetic coupling of Fe–RE magnetic moments [16]. In our case, Tb and Fe are coupled antiferromagnetically which leads to a relatively low value of the remanence induction B_r (about 0.27 T) and consequently $|BH|_{max}$ (about 10 kJ/m^3). Apart from that, the studied family of alloys can be considered as magnetically stable high-coercive materials.

The aim of this work is to study the influence of Nb content on the phase structure and magnetic properties of $(Fe_{86-x}Nb_xB_{14})_{0.88}Tb_{0.12}$ ($2 \leqslant x \leqslant 8$) bulk nanocrystalline alloys prepared using the vacuum mold suction technique. The niobium variation was chosen considering the fact that in amorphous alloys, an Nb addition slows down diffusion of iron [17], which, in a combination with a specific cooling rate during the casting procedure, may affect contents of different phases, microstructure and consequently magnetic properties of the examined alloys.

2. Experimental procedure

Samples of $(Fe_{86-x}Nb_xB_{14})_{0.88}Tb_{0.12}$ ($x = 2, 4, 6, 8$) were prepared by the mold casting technique. Each composition was made using a casting mold with the inner diameter of 1.5 mm. The applied technology consists of two steps. Firstly, a $Fe_{86-x}Nb_xB_{14}$ amorphous melt spun ribbon was melted with a proper amount of Tb element (purity of 99.96%) using a typical arc furnace in an inert gas atmosphere. In the second step, the obtained alloy ingots were cast in a copper mold using the self-designed vacuum suction apparatus [18]. Additionally, in order to find optimal casting parameters, melting current was changed from 15 to 40 A.

Phase identification was performed with the use of X-ray diffraction (XRD in an h–2h Siemens D-5000 diffractometer using Cu Kα radiation (1.5418 Å)). Magnetic measurements were carried out by using a SQUID magnetometer (XL-7, Quantum Design) in the temperature range of 300–750 K and magnetic field up to 7 T.

Observation of magnetic domains was carried out by the means of magnetic force microscopy (MFM) using a Quesant Q-Scope 250 AFM/MFM system, equipped with a 40 μm × 40 μm piezo-scanner. For these measurements, the samples were included into a resin and then mechanically polished. MFM images were collected with the silicon probe coated by a 40 nm thick cobalt alloy film. The cantilever resonant frequency and its force constant were about 75 kHz, and 2.8 N m^{-1}, respectively. Microstructural characterization of the sample surfaces as well as chemical analysis were performed using scanning electron microscopy SEM and energy-dispersive X-ray spectroscopy EDS (JEOL – JSM 6480).

3. Results

The samples of $(Fe_{80}Nb_6B_{14})_{0.88}Tb_{0.12}$ alloy were prepared using different melting currents I ranging from 15 to 45 A. Hysteresis loops determined at room temperature, displayed in Fig. 1, show that the magnetic saturation slightly decreases while the coercive field H_c significantly increases with the increasing I value. The highest H_c equal to 5.7 T was observed for $I = 35$ A. Microstructure of the alloys were studied by means of SEM and EDS techniques. Fig. 2 shows SEM images (in SEI mode and with magnifications of 500 and 2000) collected for the $(Fe_{80}Nb_6B_{14})_{0.88}Tb_{0.12}$ alloys prepared using melting currents of 15 and 35 A. Application of current $I = 35$ A results in formation of dendrite-like grains. Dimensions of the grains are smaller in the outer part of the rod, what is probably related to a higher cooling rate near the inner surface of the used copper mold. In the case of $I = 15$ A, a relatively weak contrast, suggesting only some chemical separations, is observed. More detailed analysis were performed using the EDS technique. Fig. 3 shows a SEM BSE image as well as element maps of Nb, Fe and Tb for $(Fe_{80}Nb_6B_{14})_{0.88}Tb_{0.12}$ alloy prepared using a melting current $I = 35$ A, which corresponds to the highest value of H_c. For clarity, the red contours, indicating some areas, are plotted in the same places in each figures. The obtained results indicate that the dendritic grains (bright area in the SEM image) are composed of Fe and Tb, surely forming the $Tb_2Fe_{14}B$ phase, while the area between the dendrite branches consist of Nb. A similar microstructure was found for $I = 45$ A. In the case of the lower melting current, the situation is completely different. As shown in Fig. 4, for $I = 15$ A, some Nb (dark marks) and Tb (white marks) separations are detected. Accounting the observed maximum of H_c, (refer to Fig. 1), a further analysis, related to the influence of Nb content on structural and magnetic properties, was carried out for the alloys prepared using the melting current equal to 35 A.

Crystal structure of the $(Fe_{86-x}Nb_xB_{14})_{0.88}Tb_{0.12}$ ($2 \leqslant x \leqslant 8$) bulk alloys was also studied by means of the XRD technique. Fig. 5

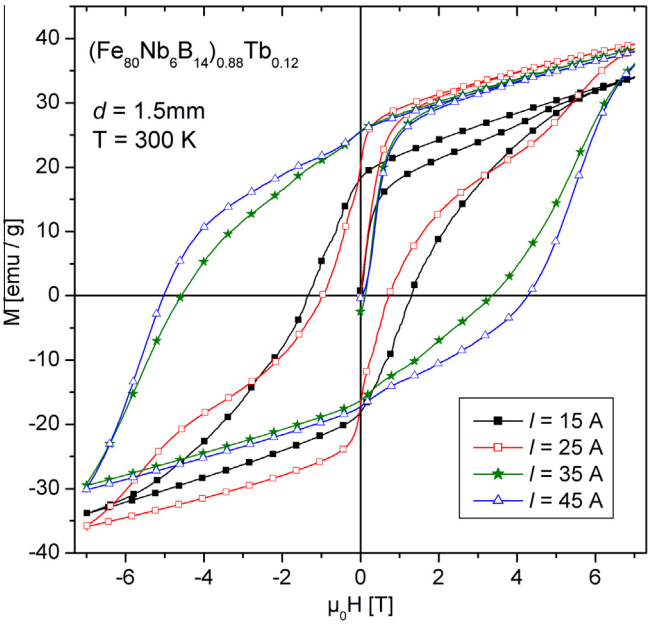

Fig. 1. Hysteresis loops for the $(Fe_{80}Nb_6B_{14})_{0.88}Tb_{0.12}$ alloys prepared with different melting currents I.